Electrochimica Acta 174 (2015) 480–487

Contents lists available at ScienceDirect

Electrochimica Acta

journal homepage: www.elsevier.com/locate/electacta

Gluconic Acid Synthesis in an Electroenzymatic Reactor

M. Varničić[a], T. Vidaković-Koch[a,*], K. Sundmacher[a,b]

[a] Max Planck Institute for Dynamics of Complex Technical Systems, Sandtorstraße 1, D-39106 Magdeburg, Germany
[b] Otto-von-Guericke University Magdeburg, Process Systems Engineering, Universitätsplatz 2, D-39106 Magdeburg, Germany

ARTICLE INFO

Article history:
Received 17 March 2015
Received in revised form 26 May 2015
Accepted 26 May 2015
Available online 9 June 2015

Keywords:
Electroenzymatic reactor
Glucose Oxidase
3-D enzymatic electrodes
Horseradish Peroxidase
Gluconic Acid

ABSTRACT

Glucose was selectively oxidized to gluconic acid in a membraneless, flow-through electroenzymatic reactor operated in the mode of co-generating chemicals and electrical energy. At the anode the enzyme glucose oxidase (GOx) in combination with the redox mediator tetrathiafulvalene (TTF) was used as catalyst, while the cathode was equipped with an enzyme cascade consisting of GOx and horseradish peroxidase (HRP). The influence of the electrode preparation procedure, the structural and the operating parameters on the reactor performance was investigated in detail. Under optimized conditions, an open circuit potential of 0.75 V, a current density of 0.6 mA cm^{-2} and a power density of 100 μA cm^{-2} were measured. The space time yield of gluconic acid achieved at a glucose conversion of 47% was 18.2 g h^{-1} cm^{-2}.

1. Introduction

Electroenzymatic processes combine the high selectivity of enzymatic catalysts with the electrochemical regeneration of their co-factors. This conceptual approach seems to be very promising for development of new biotechnological production processes [1–3]. In the present work the potential of a novel electroenzymatic reactor for the production of gluconic acid has been evaluated. Gluconic acid is a mild organic acid with applications in different industrial branches. It belongs to the commodities with an annual production of 100.000 t [4–6]. It can be obtained by partial oxidation of glucose. Glucose itself can be considered as one a renewable platform chemical [7].

Up to now, several electroenzymatic processes for gluconic acid production have been described. One of the first works in this direction was reported by Bourdillon et al. in the late 1980s [8]. Further developments of this route are listed in Table 1. Most of the described processes operate at pH 7 and a temperature of T = 30 °C or room temperature, since under these conditions enzymatic catalysts (glucose oxidase and glucose dehydrogenase) show the highest activity. Although the applied reactor configurations are quite different, there is a clear trend towards membrane reactors. Two types of membrane reactors were used. The first type implements dialysis membranes [9], while the second type uses ion-exchange (e.g. Nafion) membranes [10,11]. The mechanisms of enzyme regeneration in these two reactor types are essentially different. Reactors employing a dialysis membrane rely upon biochemical enzyme regeneration with oxygen as electron acceptor. The role of electrochemistry is the removal of hydrogen peroxide formed as a by-product of biochemical enzyme regeneration. It was shown that such an electroenzymatic process is 50% more efficient than a comparable non-electrochemical enzymatic process performed with the same quantity of enzymes [12]. Opposite to this, reactors with Nafion membrane rely upon electrochemical regeneration of co-factor, avoiding oxygen as natural electron acceptor. In these reactors, it is more common to use enzyme glucose-dehydrogenase than glucose oxidase, since the first one depends on soluble co-factor nicotinamide adenine dinucleotide (NAD), while the second one on tightly bounded flavin adenine dinucleotide (FAD) as the co-factor. The electrochemical regeneration of the co-factor was achieved with the help of different mediators (e.g. 3,4–dihydroxybenzaldehyde or phenazine methosulfate [11,13–15]. Most systems were operated in a semi-batch mode with total volumes in the range between 10 and 200 ml and electrode surface areas between 3 and 30 cm^2. The glucose concentrations ranged from 10 to 248 mM, where the majority of authors used lower concentration levels (Table 1). In most of the published works, as counter electrode materials platinum [9,12] or a carbon felt [10,11] were used. The glucose conversions in these reactors varied from 30 to 85 % at electrolysis times between 3 and 12 h.

So far, all proposed electroenzymatic processes are running non-spontaneously, i.e. they require external input of electrical energy for continuous operation. In the present work, the proposed process configuration operates in the co-generation mode, thus the process is running spontaneously like a fuel cell. Additionally, this

* Corresponding author.

http://dx.doi.org/10.1016/j.electacta.2015.05.151

Table 1
An overview of electroenzymatic processes for gluconic acid production.

System	Enzyme	Enzyme Immobiliza-tion	Electron transfer	Electrode surface area / cm^2	Volume / cm^3	Glucose concentra-tion / mM	Time / h	Glucose Conver-sion / %	STY / $g\,h^{-1}\,cm^{-2}$	Ref.
Membrane (Nafion)	GDH	In solution	direct	24	28	10	12	85	0.16	[10]
Membrane (Nafion)	GDH	Covalent attachment	Mediated (3,4–DHB)	24	28	100	4	60	3.43	[11]
Membrane (Dialysis)	GOx	Entrapment in dialysis membrane	Mediated (O_2)	30	44	248	3	30	7.13	[9]
Batch	GOx	In polypyrrole film	Mediated (O_2)	3.14	10	20	8	62	0.97	[12]
RDE system	G6PDH	Covalent attachment	Mediated (PMS)	19.6	200	9.3	6	43	1.33	[13]
Membrane-less	GOx	3-D electrode	Mediated (TTF, O_2)	1	70	20	7	47	18.2	This Work

Abbreviations: GDH– glucose dehydrogenase; G6PDH– glucose-6-phosphat-dehydrogenase; GOx – glucose oxidase; NAD– nicotinamide adenine dinucleotide; NADP– nicotinamide adenine dinucleotide phosphate; TTF – Tetrathiafulvalene; 3, 4–DHB- 3, 4-dihydroxybenzaldehyde; PMS– phenazine methosulfate

variant is completely based on enzymatic catalysts (both anode and cathode), all catalysts and the mediator are immobilized and the reactor employs no membrane (Fig. 1). Tetrathiafulvalene (TTF) has been applied as mediator for GOx regeneration on the anode side, while on the cathode side a GOx - horseradish peroxide (HRP) cascade has been implemented. By this enzyme cascade, glucose is first oxidized giving hydrogen peroxide, which is then further reduced to water, while HRP is regenerated electrochemically. In this way electrons are released on the cathode side, and the by-product hydrogen peroxide is locally removed, which should increase the stability of the enzyme GOx. The presence of GOx on both electrodes increases the space time yield of the gluconic acid. This is major advantage of enzymatic cascade on the cathode side, compared to the utilization of a single enzyme like Bilirubin oxidase (BOD). In the present contribution, feasibility of proposed electroenzymatic reactor for glucose oxidation to gluconic acid has

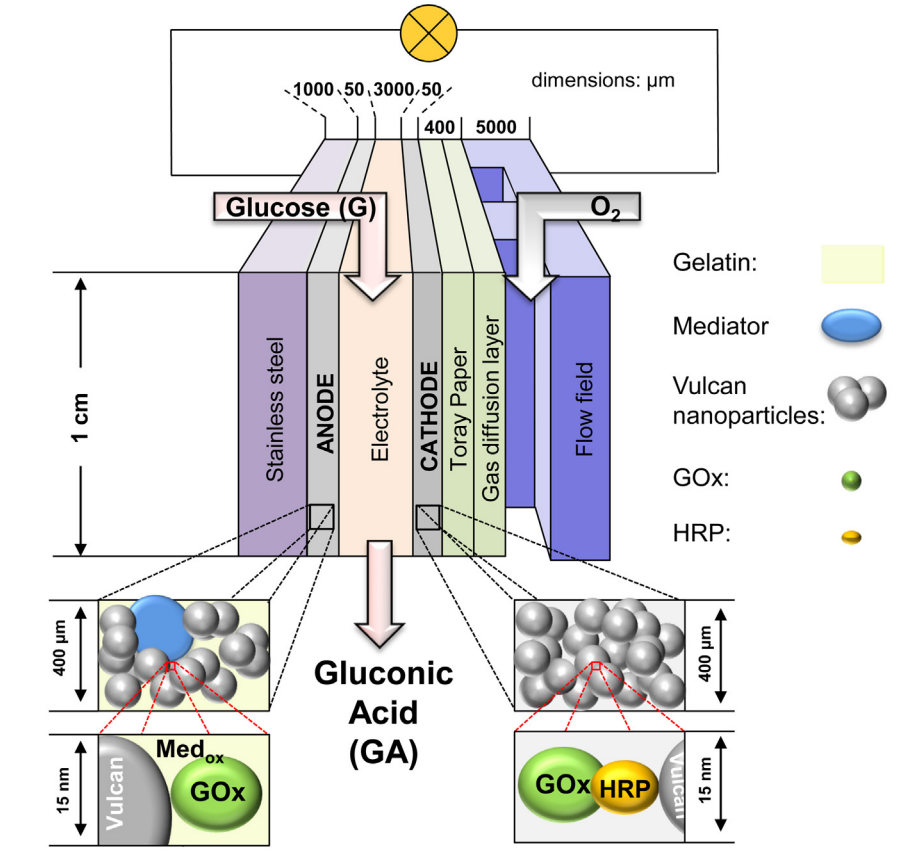

A1: $G + GOx_{ox} \leftrightarrow GA + GOx_{red}$
A2: $Med_{ox} + GOx_{red} \leftrightarrow Med_{red} + GOx_{ox} + 2H^+$
A3: $Med_{red} \leftrightarrow Med_{ox} + 2e^-$

C1: $G + GOx_{ox} \leftrightarrow GA + GOx_{red}$
C2: $Gox_{red} + O_2 \leftrightarrow H_2O_2 + GOx_{ox}$
C3: $H_2O_2 + HRP_{red} \leftrightarrow H_2O + HRP_{ox}$
C4: $HRP_{ox} + 2e^- + 2H^+ \leftrightarrow HRP_{red}$

Fig. 1. Schematic representation of electroenzymatic reactor, with anode and cathode reactions mechanisms.

been investigated. The influence of the structural and operational parameters on glucose conversion has been studied.

2. Experimental part

2.1. Chemicals and materials

Glucose oxidase (EC 1.1.3.4, GOx) from *Aspergillus niger* and Horseradish peroxidase (EC 1.11.1.7, HRP) from *Amorica rusticana* were supplied from Fluka and Serva Electrophoresis GmbH, respectively.

Gelatin for microbiology was purchased from Merck. All other chemicals including poly(vinylidene fluoride) (PVDF), glutaraldehyde (GA), 1-methyle-2-pyrrolidone, glucose and tetrathiafulvalene (TTF) were from Sigma-Aldrich. For preparation of all solutions, Millipore water was used.

Vulcan nanomaterial was supplied by Cabot Corporation. Spectroscopically pure carbon rods supplied by Ted Pella, 330 INC, USA were cut in 11 mm diameter discs. Non-treated (in text hydrophilic) Toray paper (type: TGP-H-060) was purchased from Toray Deutschland GmbH. To obtain hydrophobic Toray paper, non-treated Toray paper was immersed in 25.1% of polytetrafluuoroethylene (PTFE) emulsion for 60 min and after that dried in the oven at 90 °C.

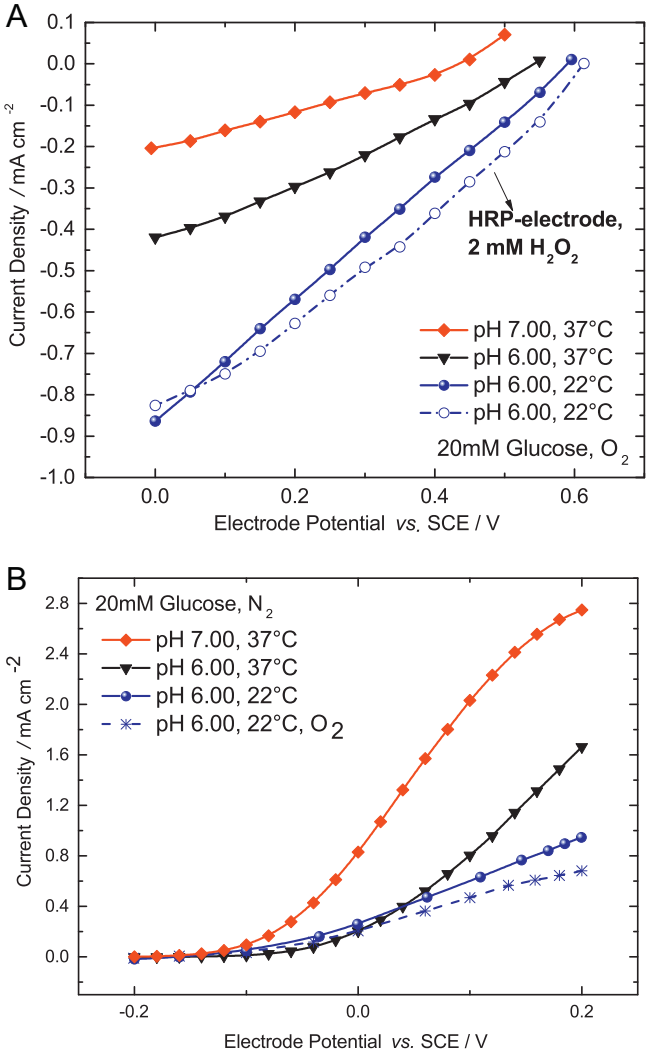

Fig. 2. Steady state performances of a) enzymatic cathode (GOx-HRP or HRP) and b) enzymatic anode (GOx/TTF) at two different pH and temperatures. Conditions: half-cell measurements, enzyme immobilization: cathode, Vulcan-PVDF; anode, Vulcan-Gelatin, rotation rate: 400 rpm.

2.2. Preparation of enzymatic electrodes

Enzymatic anodes were prepared by using the Vulcan-Gelatin procedure described previously by Ivanov et al. [16]. At first, 2% of gelatin solution in distillated water was prepared by heating the solution up to 37 °C in order that gelatin powder dissolves. After that, 20 mg of carbon nanoparticles, 10 mg of enzyme (GOx) and 10 mg of TTF mediator were suspended in 1 ml of gelatin solution (2%, 37 °C) and cast on the stainless steel supports with the geometrical surface areas of 0.28 cm^2 (for applications in the half-cell) or 1 cm^2 (for use in the reactor). The electrodes were then cross linked by dipping for 60 s in the solution of 5 % glutaraldehyde. Finally, cross-linked electrodes were rinsed with plenty of distillated water, left to dry at room temperature and stored in the fridge at -18 °C before further use. Enzymatic cathodes were prepared following two different procedures. One procedure was similar to the already described Vulcan-Gelatin procedure, with the exception that instead of pure GOx, a mixture of GOx and HRP with the optimized ratio of 1:3 was applied. The second procedure was similar to the Vulcan-PVDF procedure reported by Varnicic et al. [17]. According to this procedure, Vulcan nanomaterial was suspended in 0.25% solution of PVDF in 1-methyle-2-pyrrolidone. The ink was then cast on the spectroscopically pure graphite support (SPG) with 0.28 cm^2 geometrical surface area (for half-cell experiments) or Toray paper with 1 cm^2 (for reactor experiments). The prepared electrodes were dried at 60 °C. After drying and cooling down the electrodes to room temperature, the enzyme solution of GOx and HRP in 0.1 M phosphate buffer (1:3) was put and left to adsorb with different adsorption time (2 h or 18 h at 4 °C). Subsequently, the prepared electrodes were rinsed with buffer and were ready for electrochemical measurements.

2.3. Electroenzymatic reactor

The used electrochemical reactor was a membrane-less, flow-through device. Enzymatic anode and cathode were separated by a single channel of 3 mm width. The reactor was mounted vertically in an appropriate holder and glucose solution was recirculated from well-mixed reservoir (V_r = 70 ml) with a flow rate of 10 ml min^{-1}. Oxygen was supplied to the cathode side from the gas phase (flow rate ca. 500 ml min^{-1}). On the cathode side, a double layer of Toray paper was implemented. One layer was hydrophilic and it was serving as a support for the catalyst layer. The second layer was hydrophobic. It served as a gas diffusion layer and was directly contacted with the graphite flow field. The scheme of the electroenzymatic reactor is shown in Fig. 1. The glucose concentration was 20 mM. All reactor experiments were performed at pH 6.0 in 0.1 M phosphate buffer at room temperature.

Table 2
Vulcan and enzyme loadings of enzymatic cathodes.

System	Vulcan Loading/mg cm^{-2}	Enzyme Loading (adsorption time) / h
Reactor 1	2	2
Reactor 2	4	2
Reactor 3	4	18

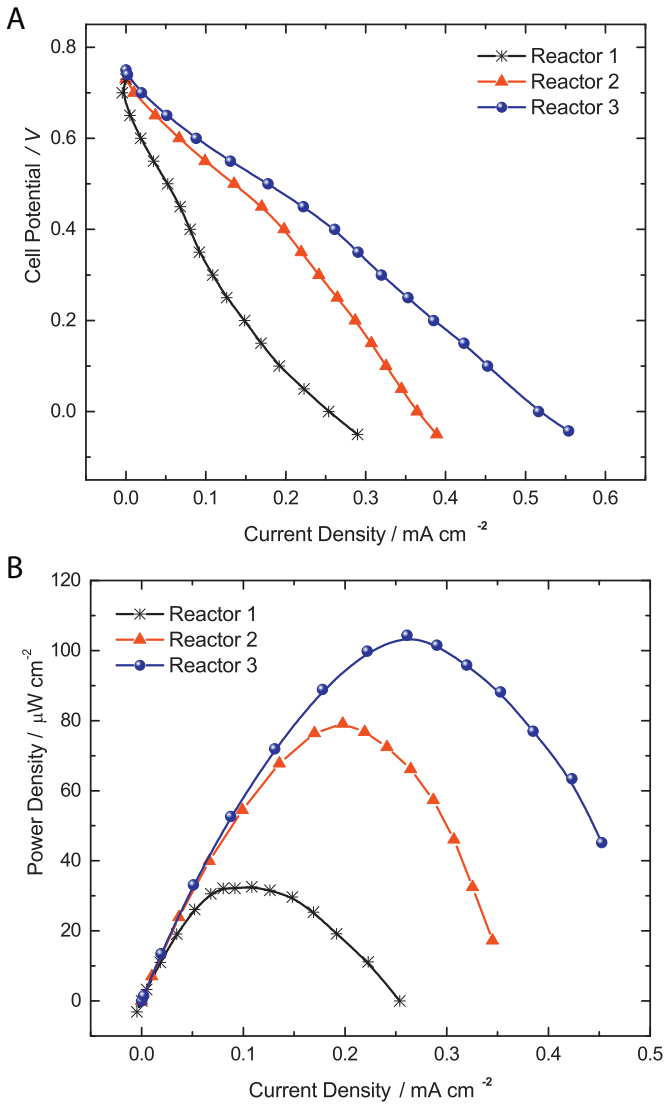

Fig. 3. a) Polarization and b) power curves of electroenzymatic reactors employing GOx/TTF anode and GOx-HRP cathodes; Conditions: enzyme immobilization: cathode, Vulcan-PVDF; anode, Vulcan-Gelatin, 20 mM glucose in 0.1 M phosphate buffer, 10 ml min^{-1} flow rate, O_2 supply from the gas phase, pH 6.00, 22 °C, volume of the glucose reservoir: 70 ml.

2.4. Measurements

Electrochemical half-cell and reactor tests were performed using the Autolab potentiostat PGSTAT302 (Eco Chemie). The reactor was connected as a 2-electrode system to the potentiostat. The anode and cathode potentials were monitored under operating conditions with the help of external voltmeters connected to the RE. Half-cell experiments were carried out in the 3-electrode configuration with a rotating disc electrode (RDE, Radiometer Analytical, model ED101). Enzymatic electrodes were used as working, Pt as counter and saturated calomel electrode (SCE) as reference electrode. All experiments were performed in 20 mM glucose in 0.1 M phosphate buffer prepared at least one day before starting the measurements. The experiments were performed at pH 6 or 7 and room temperature or T = 37 °C. Steady state polarization data were extracted from chronopotentiostatic measurements by taking the current value after 120 s at each constant potential value.

The glucose concentration was measured spectrophotometrically (UV/Vis spectrophotometer, SPECORD S600, Analytikjena, Jena, Germany) using glucose assay kits (UV-test, R-Biopharm, Darmstadt, Germany). Every hour a small aliquot was taken from the glucose reservoir in order to control the glucose concentration.

3. Results and Discussion

3.1. Electrode preparation procedure and operating conditions

In our previous publication [17] two procedures for the preparation of enzymatic electrodes were described. In one of these, gelatin was used as a binder and electrodes were cross-linked, while in the other procedure PVDF was the binder and enzymes were only adsorbed on the surface without cross-linking. In case of HRP, the PVDF procedure without cross-linking resulted in electrodes of better performances than the gelatin procedure. It was observed that cross-linking forms enzyme agglomerates, decreasing the number of enzymes in contact with electron conductive surface, leading finally to a decrease of the activity [17]. It can be expected that this problem will always occur for Direct Electron Transfer (DET) enzymes. Since the cathode (GOx-HRP) in the present set-up relies upon DET, one can expect that the Vulcan-PVDF procedure will be more advantageous than the Vulcan-Gelatin procedure. Indeed, this has been confirmed (please see Supporting information, Fig. S1), which motivated the use of the Vulcan-PVDF procedure for the preparation of the enzymatic cathode in the present work. Up to now, the GOx-HRP combination has been mainly studied for biosensor applications where emphasis was on the electrode sensitivity and not on the utilization of high glucose concentrations and electrode performance in terms of current densities [18–20]. In the present case, optimized GOx-HRP electrode at 20 mM glucose can reach current densities of up to 0.9 mA cm^{-2}, which is comparable with performances reported for laccase or bilirubin oxidase enzymatic electrodes used in enzymatic fuel cell application (taking into account that 2 instead of 4 electrons are exchanged in the fuel cell case) [21–25]. The enzymatic cathode comprising the GOx-HRP cascade has similar performance as the HRP cathode prepared with the same procedure in the presence of 2 mM hydrogen peroxide (Fig. 2a). For the enzymatic anode, it was shown that in both procedures similar limiting currents can be reached, while the Vulcan-Gelatin procedure shows more negative onset potentials compared to the Vulcan-PVDF procedure (please see Fig. S2 in

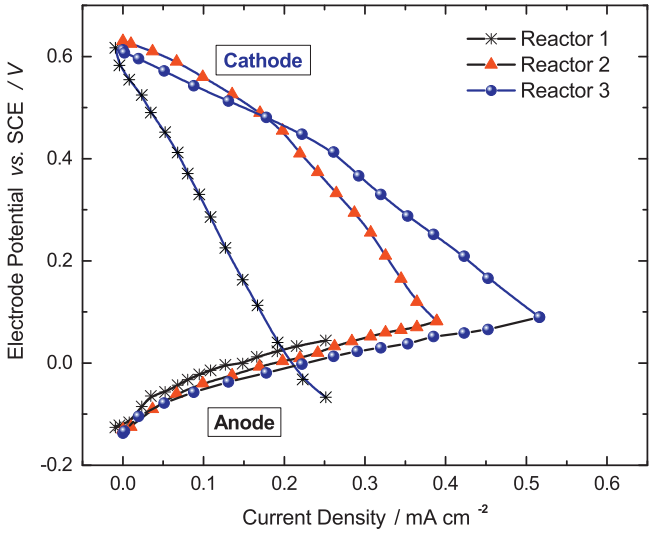

Fig. 4. Steady state performances of enzymatic cathode (GOx-HRP) and enzymatic anode (GOx/TTF) under operations conditions in enzymatic reactor. Conditions as in Fig. 3.

Supporting information). Based on this experience, the Vulcan-Gelatin procedure has been chosen for preparation of the enzymatic anode in the reactor.

After the electrode preparation procedures was establihsed, operating conditions (pH and temperature) in the reactor were investigated. These conditions largely depend on the optimal pH level and temperature at which enzymatic catalysts show their optimal activity. According to the literature, optimal conditions for GOx are pH 5.0 to 8.0 and a temperature of T = 37 °C [26–29], while for HRP pH 6.0 to 7.0 and T = 22 °C were found to be optimal [30–32]. The dependency of these conditions on the enzyme immobilization procedure can be seen in Fig. 2. The results show different optima for anode and cathode sides (pH 7 and T = 37 °C on the anode side; pH 6 and T = 22 °C on the cathode side). As seen in Fig. 2, changing of pH and temperature can also influence the onset electrode potential. For optimal cathode conditions, peroxide reduction starts at 0.6 V vs. SCE which corresponds well to the literature value for peroxide reduction on HRP-loaded graphite electrodes [33]. The onset potential of enzymatic electrode with the mediator TTF is around -0.15 V vs. SCE which is slightly more negative than the onset potential of other electrodes using TTF as mediator (around -0.1 V vs. SCE) [34,35]. The membrane-less reactor configuration in the present work requires a compromise regarding pH, temperature and composition of the electrolyte. In the present case, lower pH and temperature were chosen since the whole system is limited electrochemically by the cathode. Regarding the composition of the electrolyte, the main issue is the presence of oxygen which, as natural electron acceptor for GOx, competes with TTF as electron acceptor on the anode side (Fig. 2b). This reduces the achievable current level in the system, since part of the electronic current is lost. But this phenomenon does not influence the conversion of glucose. Still some hydrogen peroxide evolves on the anode side, which possibly decreases the anode stability. There are several approaches to tackle this issue. First, the impact of oxygen is more pronounced at more positive over-potentials (Fig. 2b), which means that careful selection of the operating potential of the anode can reduce this problem. Second, in the present reactor configuration oxygen can be supplied a) only from the gas phase, b) from the gas phase and from the solution, or c) only from the solution (Fig. 1). In the following experiments oxygen supply only from the gas phase through gas diffusion layer was applied. In this way, merely non-reacted oxygen on the cathode side might reach the anode side and react there.

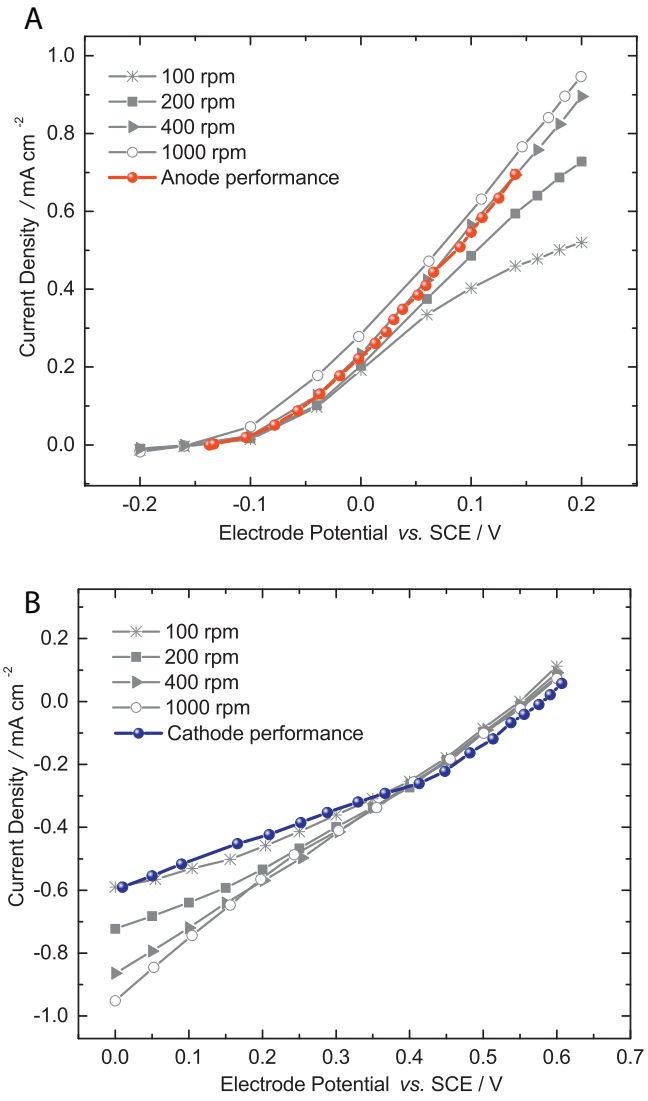

Fig. 5. Comparison between steady state performances of a) enzymatic anode (GOx/TTF) and b) enzymatic cathode (GOx/HRP) tested in half-cell and electro-enzymatic reactor. Conditions: enzyme immobilization: cathode, Vulcan-PVDF; anode, Vulcan-Gelatin, 20 mM glucose in 0.1 M phosphate buffer, pH 6.00, 22 °C. Flow rates: 10 ml min^{-1} for glucose solution, O_2 supply from the gas phase in the reactor; rotation rates between 100 and 1000 rpm in the half-cell.

3.2. Investigation of electroenzymatic reactor performance

Electroenzymatic reactor in the present work has similarities with the previously reported fuel cell device reported by Ivanov et al. [17]. Moreover, the new electroenzymatic reactor was equipped with a reference electrode in order to monitor (and control) electrode potentials under operating conditions. This enabled both the voltastatic and the potentiostatic mode of operation. The influence of the structural parameters on the electrochemical performance of the enzymatic reactor and glucose conversion was investigated in detail. As structural parameters the enzyme and Vulcan nanoparticle loadings on the cathode side were varied, while the parameters of the enzymatic anode were kept constant.

3.2.1. Electrochemical performance

Two cathode structural parameters were changed: a) Vulcan loading, and b) enzyme loading (Table 2). The Vulcan loading determines the available surface area for catalyst adsorption, electrochemical surface reactions and charge transfer. Loadings of 2 and 4 mg cm^{-2} were tested. The further increase of the loading was not possible due to mechanical instability of the electrode. The enzyme loading was varied by changing the adsorption time between 2 and 18 h. After 18 h, saturation conditions were reached and the electrode activity was not further changing. The obtained polarization and power density curves of the electroenzymatic reactors employing different cathodes are presented in Fig. 3. As can be seen, the open circuit cell potential was around 0.75 V. This value was found to be independent on Vulcan and enzyme loadings, and this is in good correlation to the value obtained at open circuit potentials of single electrodes (-0.15 V and 0.6 V vs. SCE, for anode and cathode, respectively). Different open-circuit cell potentials were reported in the literature for other glucose/oxygen biofuel cells. This depends mainly on the choice of enzymes used for the cathode side (typically BOD or laccase), and on the choice of the mediator used for GOx regeneration on the anode. The reported values in literature range from 0.45 V for the fuel cell following similar idea as in the present paper but, with phenanthroline as GOx mediator [36] to 0.9 V for the Osmium redox hydrogels as GOx mediator [37,38]. In general, the investigated electrochemical cell shows a high open circuit cell

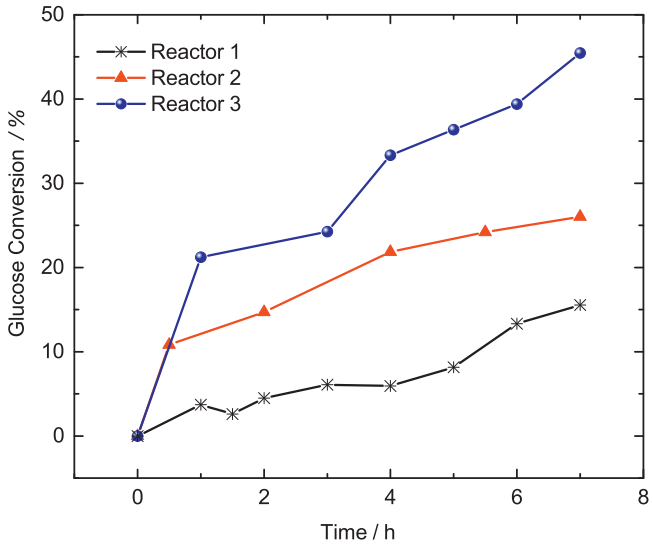

Fig. 6. Glucose conversion during 7 h in electroenzymatic reactors.

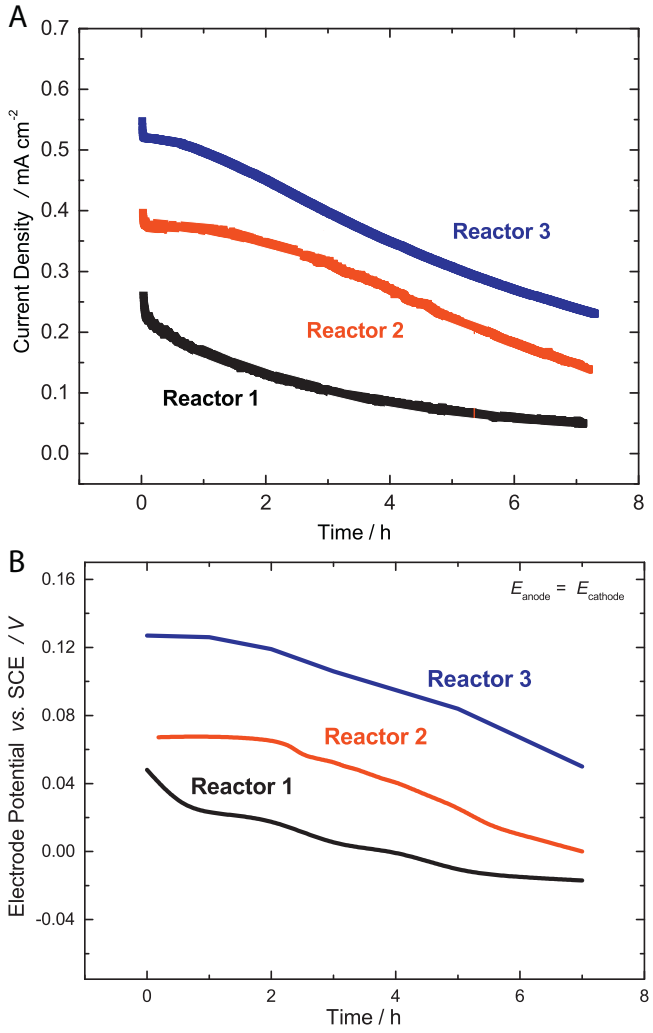

Fig. 7. a) Current density change during 7 h of reactor operation under voltastatic conditions (U_{cell} = 0.0 V) and b) change of anode and cathode electrode potentials during reactors operation (for further explanations please see the text).

potential. As can be seen in Fig. 3, the increase of Vulcan and enzyme loadings improves the performance of the fuel cell significantly, both in terms of current density and power output (from ca. 300 μA cm^{-2} to ca. 600 μA cm^{-2} and ca. 30 to 100 μW cm^{-2}, respectively). The power density of the here presented Reactor 3 can be compared to other glucose/oxygen fuel cells based on GOx and BOD or laccase as cathode [39–44]. The performance of our reactor is superior compared to the enzymatic fuel cell with the same combination of enzymes and a maximum power density of around 5 μW cm^{-2} for 20 mM glucose solution [36]. But this power level is clearly below the performance of the so far reported best performance of enzymatic fuel cells [45].

The presence of the reference electrode in the present set-up enables to distinguish between losses on cathode and anode sides separately. As can be seen in Fig. 4 the overpotential on the cathode side is more significant than on the anode side, with the cathode limiting the performance of the whole fuel cell. The increase of the Vulcan loading (from 2 to 4 mg cm^{-2}) between Reactors 1 and 2 causes a significant decrease of the cathodic overpotential at the same current density. This allows much higher current densities to be reached. In these experiments the enzyme adsorption time was kept constant, but one can expect a higher enzyme loading in Reactor 2 than in the Reactor 1, due to higher available surface area for the adsorption. The difference between Reactor 2 and 3 is in enzyme adsorption time on the cathode side, which reflects the higher enzyme loading. It can be seen that at lower overpotential, the cathode in Reactor 2 performs a bit better than in Reactor 3, while at higher overpotential, the cathode with higher enzyme loading performs better. This can be as an indication for HRP inhibition in Reactor 3 at low overpotentials due to mismatch between the production and consumption rates of hydrogen peroxide (reaction C2 in Fig. 1; reaction C3 in Fig. 1). While the former reaction is influenced only by the enzyme loading, species concentration and flow conditions, the latter one can be accelerated electrochemically via higher currents in Reactor 3 at more negative overpotentials than in Reactor 2 [9].

At the same time, the enzymatic anode shows a moderate decrease of the overpotential between Reactors 1, 2 and 3 (Fig. 4). Although these differences can be due to deviations between single experiments, this change appears to be not a random effect, but a clear trend. A possible reason for this increase of the anode overpotential can be the presence of oxygen in the solution. Oxygen is a natural electron acceptor for GOx and thus it competes with TTF for electrons, causing a decrease of the anode current in the presence of oxygen i.e. an increase of anode overpotential at the same current density. As already discussed, in all experiments oxygen was supplied from the gas phase and it was initially not present in the liquid phase. The amount of oxygen in the liquid phase is governed by the interplay of oxygen supply to the cathode catalyst layer, oxygen consumption by the enzymatic reaction and diffusion of non-reacted oxygen away from the catalyst layer. Due to concentration gradients, one can expect that non-reacted oxygen will diffuse out to the liquid phase. If convection-diffusion conditions in the liquid phase allow it, oxygen can finally reach the anode and react there enzymatically. The amount of oxygen reaching the anode for the same flow conditions in the gas and liquid phase is mainly influenced by the properties of the cathode catalyst layer, i.e. basically by oxygen consumption in the catalyst layer. The results in Fig. 4 indicate higher oxygen consumption in Reactor 3 compared to Reactor 1, suggesting a lower influence of oxygen cross-over in Reactor 3 than in the Reactor 1.

While it was reported that the performance of enzymatic electrodes tested in the 3- and 2-electrode set-ups can differ significantly (e.g. BOD-cathode reached 5 mA cm^{-2} in the 3-electrode set-up, but only 200 μW cm^{-2} in the 2-electrode set up in presence of 50 mM glucose and at 37 °C and pH 7.2 [39]), no significant difference was observed in the present study. To assure direct comparison, the performance of anode and cathode in the 2-

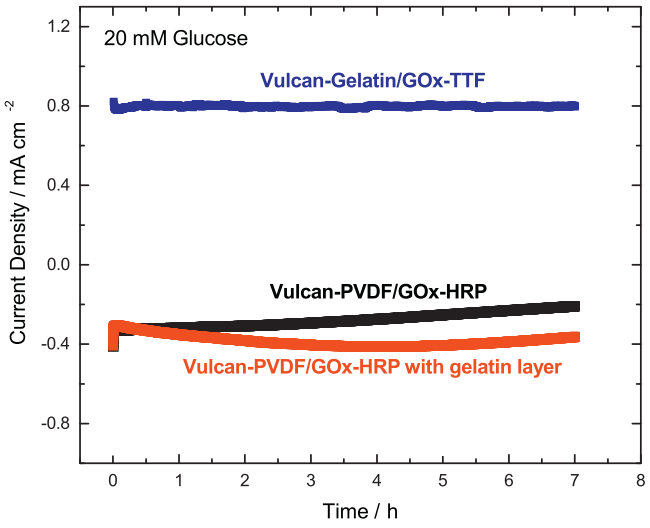

Fig. 8. Performances of enzymatic electrodes during 7 h of testing. Conditions: half-cell measurements, enzyme immobilization: cathode, Vulcan-PVDF; anode, Vulcan-Gelatin, 20 mM glucose in 0.1 M phosphate buffer, pH 6.00, 22 °C, rotation rates 400 rpm, potential of the electrodes: 0.15 V vs. SCE.

Table 3
Glucose conversion after 7 h in different reactors.

System	Total Conversion / %	Electrochemical part of conversion / %	Enzymatic part of conversion / %
Reactor 1	16	14	86
Reactor 2	30	19	81
Reactor 3	47	17	83

electrode set-up (Reactor 3) was plotted against the anode and cathode being characterized separately in the 3-electrode set-up (Fig. 5). The electrodes were always prepared via the same procedure. The experimental data indicate no significant scaling issues (0.28 and 1 cm^2 for 3- and 2-electrode set-up, respectively). Some differences can be explained by different flow conditions applied in the two different set-ups (rotating disc electrode in 3-electrode set-up, compared to flow-through reactor in the 2-electrode set-up).

3.2.2. Glucose conversion

The glucose concentration over time of electrolysis has been followed by taking a sample every hour and by determining glucose concentration with a help of assay kits. The conversion has been calculated as the ration of the converted amount of glucose to amount of glucose at the beginning of electrolysis. The glucose conversions during 7 h of operation in the electroenzymatic reactor under voltastatic conditions (U_{cell} = 0.0 V) are shown in Fig. 6. The cumulative conversion increases from 16% (Reactor 1) to 47% (Reactor 3). One obvious reason for this finding is an improved enzymatic cathode which allows the reactor to operate at higher current density. The change of cell currents during voltastatic operation is shown in Fig 7a, while the change of electrode potentials is given in Fig. 7b. As can be seen, Reactor 3 operates at higher current densities than Reactors 1 and 2, which is also reflected by higher glucose conversion. The enzymatic anode in the Reactor 3 exerts higher overpotentials than the anodes in Reactors 1 and 2. Since the operating cell potential in all cases was U_{cell} = 0, the cathode and anode potentials are identical (Fig. 7b). The progress of anode and cathode overpotentials goes into different directions with the anode overpotential decreasing over time and the cathode overpotential increasing. This might be an indication that the cathode performance deteriorates over time. To check this, anode and cathode were investigated in a differential reactor (to avoid the effect of glucose concentration variation in the batch reactor). The results in Fig. 8 show that the enzymatic anode is indeed very stable, while the enzymatic cathode shows a decrease of activity of ca. 25% over time. This loss can be attributed to the above mentioned enzyme inhibition effect or the leaching out of enzymes. In the present case, it seems that the leaching out effect dominates since the formation of gelatin film on the top of enzymatic cathode resulted in almost no loss of activity during the same time (Fig. 8).

In electrochemical systems the reactant conversion can be calculated from the electric charge passed into the reactor during a certain time, by use of Faraday's law. For this calculation a certain current efficiency for a single reaction has to be assumed. Presuming 100% current efficiency for glucose conversion, electrochemical glucose conversion has been calculated from electrical charge passed during 7 h of operation (obtained by integration of curves in Fig. 7a) and by knowing the number of exchanged electrons (2). This number has been further multiplied by 2, accounting for an glucose conversion caused by cathodic reaction. The results are shown in Table 3 in terms of the percentage of glucose converted electrochemically. Obviously, only a small part of the cumulative conversion is purely electrochemical; the larger part is probably enzymatic. It can be expected that the pure enzymatic conversion mainly takes place on the cathode side and that only a small part of this conversion takes place on the anode side. Such large enzymatic conversion on the cathode side indicates the formation of a large amount of hydrogen peroxide at the cathode side which is not further utilized by the HRP enzyme. Having the distractive nature of this by-product in mind, this issue should be studied in more detail in future. The first tests (Fig. 8) indicate no significant degradation during 7 h of operation.

3.2.3. Comparison with literature data

As already discussed, all electroenzymatic reactors proposed so far for gluconic acid production need external energy input. It can also be seen in Table 1 that the operating conditions in these reactors were very different, having different total reaction volumes, concentrations, time of electrolysis, geometry of electrodes and conversions. It is clear that the glucose conversion is dependent on the surface area of electrodes, the total volume of the reaction solution and the operation time. In order to compare data from different experimental set-ups, these parameters are to be combined to calculate the space time yield of the reactor, i.e the mass of gluconic acid produced per unit time and per unit geometric area of the electrode ($g_{gluconicacid}\,h^{-1}\,cm^{-2}$) (Table 1). Since all listed processes are batch or semi-batch systems, the mass of product was calculated based on the total volume in the system, cumulative conversion and initial concentration of glucose. The surface area is based on the geometrical surface area and the time corresponds to the total time of electrolysis. The calculated space time yield values are listed in Table 1. As can be seen, the best process based on this analysis is not related to the highest conversion achieved. Compared to other processes, the performance of Reactor 3 (Table 3) is excellent. It indicates a high potential of this reactor concept for the future development of a new biotechnological process for the electroenzymatic production of gluconic acid from glucose.

4. Conclusions

In the present work, the feasibility of the proposed electro-enzymatic reactor for gluconic acid synthesis, operated in chemical-energy co-generation mode, is demonstrated. The membrane-less reactor design enables utilization of a single

electrolyte, thereby simplifying the design and reducing the costs of the reactor. On the other hand, optimal reactor operation requires a compromise regarding pH and temperature level, which are chosen such that the conditions are optimized for the less active enzyme (HRP in the present case). It has been shown that the immobilization technique of enzymes plays an important role for optimal reactor performance. In case of DET enzymes physical adsorption of enzymes without cross-linking should be preferred. The resulting electrodes are more active, but they suffer from lower long-term stability. It has been shown that the formation of a gelatin film on top of such electrodes improves their stability without decreasing the electrode activity. The Vulcan-Gelatin procedure used for the preparation of enzymatic anodes resulted in enzymatic electrodes of excellent activity and stability over the tested time period. A glucose conversion of 47% during 7 h batch runtime has been achieved after optimizing the cathode structural parameters. The level of conversion depends on system parameters such as electrode surface area, total reaction volume and glucose concentration, as well as operation parameters like time of electrolysis and mode of operation (potentiostatic, voltastatic or galvanostatic). Careful adjustment of these parameters can result in higher conversion values, which will be reported in our next publication. It has been shown that the major part of this conversion can be attributed to the enzymatic pathway, while the smaller part is electroenzymatic. In comparison to literature data, the proposed reactor shows high potential for the development of an industrial electroenzymatic process for gluconic acid production.

Acknowledgements

All authors gratefully acknowledge the support by the Center for Dynamic Systems (CDS) financed by the Federal State Saxony-Anhalt in Germany.

The authors are also grateful to Iva Zasheva and Bianka Stein for their support and technical assistance.

Appendix A. Supplementary data

Supplementary data associated with this article can be found, in the online version, at http://dx.doi.org/10.1016/j.electacta.2015.05.151.

References

[1] T. Krieg, A. Sydow, U. Schroeder, J. Schrader, D. Holtmann, Trends in Biotechnology 32 (2014) 645–655.
[2] C. Kohlmann, W. Märkle, S. Lütz, Journal of Molecular Catalysis B: Enzymatic 51 (2008) 57–72.
[3] R. Devaux-Basséguy, P. Gros, A. Bergel, Journal of Chemical Technology & Biotechnology 68 (1997) 389–396.
[4] I. Dencic, J. Meuldijk, D.M. Croon, V. Hessel, Journal of Flow Chemistry 1 (2011) 13–23.
[5] S. Anastassiadis, I.G. Morgunov, Recent Patents on Biotechnology 1 (2007) 167–180.
[6] S. Ramachandran, P. Fontanille, A. Pandey, C. Larroche, Food Technology and Biotechnology 44 (2006) 185–195.
[7] D.Y. Murzin, R. Leino, Chemical Engineering Research & Design 86 (2008) 1002–1010.
[8] C. Bourdillon, R. Lortie, J.M. Laval, Biotechnology and Bioengineering 31 (1988) 553–558.
[9] R. Basséguy, K. Délécouls-Servat, A. Bergel, Bioprocess and Biosystems Engineering 26 (2004) 165–168.
[10] J.M. Obón, P. Casanova, A. Manjón, V.M. Fernández, J.L. Iborra, Biotechnology Progress 13 (1997) 557–561.
[11] A. Manjón, J.M. Obón, P. Casanova, V.M. Fernández, J.L. Ilborra, Biotechnology Letters 24 (2002) 1227–1232.
[12] P. Gros, A. Bergel, AIChE Journal 51 (2005) 989–997.
[13] O. Miyawaki, T. Yano, Enzyme and Microbial Technology 15 (1993) 525–529.
[14] R. Wichmann, D. Vasic-Racki, Cofactor regeneration at the lab scale, in: Technology Transfer in Biotechnology: From Lab to Industry to Production, 2005, pp. 225-260.
[15] W. Liu, P. Wang, Biotechnology Advances 25 (2007) 369–384.
[16] I. Ivanov, T. Vidakovic-Koch, K. Sundmacher, Journal of Electroanalytical Chemistry 690 (2013) 68–73.
[17] M. Varnicic, K. Bettenbrock, D. Hermsdorf, T. Vidakovic-Koch, K. Sundmacher, RSC Advances 4 (2014) 36471–36479.
[18] Y.L. Yao, K.K. Shiu, Electroanalysis 20 (2008) 2090–2095.
[19] L. Zhu, R. Yang, J. Zhai, C. Tian, Biosensors and Bioelectronics 23 (2007) 528–535.
[20] E. Csoregi, L. Gorton, G. Markovarga, Electroanalysis 6 (1994) 925–933.
[21] J. Filip, J. Sefcovicova, P. Gemeiner, J. Tkac, Electrochimica Acta 87 (2013) 366–374.
[22] C.F. Blanford, R.S. Heath, F.A. Armstrong, Chem. Commun. (2007) 1710.
[23] S. Tsujimura, Y. Kamitaka, K. Kano, Fuel Cells 7 (2007) 463–469.
[24] A. Habrioux, T. Napporn, K. Servat, S. Tingry, K.B. Kokoh, Electrochimica Acta 55 (2010) 7701–7705.
[25] L. Hussein, S. Rubenwolf, F. von Stetten, G. Urban, R. Zengerle, M. Krueger, S. Kerzenmacher, Biosensors & Bioelectronics 26 (2011) 4133–4138.
[26] M. Snejdarkova, M. Rehak, M. Otto, Analytical Chemistry 65 (1993) 665–668.
[27] W.J. Sung, Y.H. Bae, Analytical Chemistry 72 (2000) 2177–2181.
[28] W. Zhao, J.J. Xu, C.G. Shi, H.Y. Chen, Langmuir 21 (2005) 9630–9634.
[29] B.F.Y. Yonhin, M. Smolander, T. Crompton, C.R. Lowe, Analytical Chemistry 65 (1993) 2067–2071.
[30] S. Yang, W.-Z. Jia, Q.-Y. Qian, Y.-G. Zhou, X.-H. Xia, Analytical Chemistry 81 (2009) 3478–3484.
[31] R. Andreu, E.E. Ferapontova, L. Gorton, J.J. Calvente, Journal of Physical Chemistry B 111 (2007) 469–477.
[32] T. Ruzgas, E. Csoregi, J. Emneus, L. Gorton, G. MarkoVarga, Analytica Chimica Acta 330 (1996) 123–138.
[33] E.E. Ferapontova, Electroanalysis 16 (2004) 1101–1112.
[34] E. Nazaruk, K. Sadowska, J.F. Biernat, J. Rogalski, G. Ginalska, R. Bilewicz, Analytical and Bioanalytical Chemistry 398 (2010) 1651–1660.
[35] B. Kowalewska, P.J. Kulesza, Electroanalysis 21 (2009) 351–359.
[36] V. Krikstolaityte, Y. Oztekin, J. Kuliesius, A. Ramanaviciene, Z. Yazicigil, M. Ersoz, A. Okumus, A. Kausaite-Minkstimiene, Z. Kilic, A.O. Solak, A. Makaraviciute, A. Ramanavicius, Electroanalysis 25 (2013) 2677–2683.
[37] V. Soukharev, N. Mano, A. Heller, Journal of the American Chemical Society 126 (2004) 8368–8369.
[38] N. Mano, F. Mao, W. Shin, T. Chen, A. Heller, Chemical Communications (2003) 518–519.
[39] V. Flexer, N. Brun, M. Destribats, R. Backov, N. Mano, Physical Chemistry Chemical Physics 15 (2013) 6437–6445.
[40] I. Ivanov, T. Vidakovic-Koch, K. Sundmacher, Journal of Power Sources 196 (2011) 9260–9269.
[41] R.C. Reid, F. Giroud, S.D. Minteer, B.K. Gale, Journal of the Electrochemical Society 160 (2013) H612–H619.
[42] K. MacVittie, J. Halamek, L. Halamkova, M. Southcott, W.D. Jemison, R. Lobel, E. Katz, Energy & Environmental Science 6 (2013) 81–86.
[43] A. Zebda, L. Renaud, M. Cretin, F. Pichot, C. Innocent, R. Ferrigno, S. Tingry, Electrochemistry Communications 11 (2009) 592–595.
[44] M. Southcott, K. MacVittie, J. Halamek, L. Halamkova, W.D. Jemison, R. Lobel, E. Katz, Physical Chemistry Chemical Physics 15 (2013) 6278–6283.
[45] A. Zebda, C. Gondran, A. Le Goff, M. Holzinger, P. Cinquin, S. Cosnier, Nature Communications 2 (2011) .